Anomalous cooling of the parallel velocity in seeded beams: theory and experiments

Alain Miffre, Marion Jacquey, Matthias Büchner, Gérard Trénec, Jacques Vigué

Anomalous cooling of the parallel velocity in seeded beams: theory and experiments

A. Miffre, M. Jacquey, M. Büchner, G. Trénec and J. Vigué

Laboratoire Collisions Agrégats Réactivité -IRSAMC
Université Paul Sabatier and CNRS UMR 5589
118, Route de Narbonne 31062 Toulouse Cedex, France
e-mail: jacques.vigue@irsamc.ups-tlse.fr

(Dated: June 25, 2004)

Abstract

We have found recently that, in a supersonic expansion of a mixture of two monoatomic gases, the parallel temperatures of the two gases can be very different. This effect is large if the seeded gas is highly diluted and if its atomic mass is considerably smaller than the one of the carrier gas. In the present paper, we present a complete derivation of our theoretical analysis of this effect. Our calculation is a natural extension of the existing theory of supersonic cooling to the case of a gas mixture, in the high dilution limit. Finally, we describe a set of temperature measurements made on a beam of lithium seeded in argon. Our experimental results are in very good agreement with the results of our calculation.

I. INTRODUCTION

We have recently reported [1] an unexpected cooling effect in an argon supersonic beam seeded with a small amount of lithium. The parallel temperature of lithium is smaller than the parallel temperature of argon and this effect is large, the lithium parallel temperature being three times smaller than the calculated argon parallel temperature. This effect is surprising as a common assumption is that the parallel temperatures of the seeded and carrier gas are roughly equal.

This surprising effect can be explained by an extension of the theory giving the terminal parallel temperature in supersonic beams of pure gases. This theory was developed by Anderson and Fenn in 1965 [2], by Hamel and Willis [3] in 1966, by Toennies and Winkelmann [4] in 1977 and by Beijerinck and Verster [5] in 1981. The case of binary mixtures was studied theoretically by Anderson and coworkers [6, 7], as well as by other authors who are quoted by D.R. Miller in his review [8]. The case usually considered corresponds to a heavy species seeded in a light carrier gas and the early studies established that the terminal parallel temperatures of the two species are not equal (see figure 8 of reference [7]), but the calculated temperature difference was not very large in this case. The large effect discussed here exists only for a light seeded species seeded in a heavy carrier gas and, as far as we know, this situation has not been much studied by theory or by experiment.

The basic phenomenon is due to the exchange of energy between the alkali atoms and the rare gas atoms. Two effects are important: i) the alkali-rare gas interaction has a longer range than the rare gas-rare gas interactions so that the expansion cooling goes on for a longer time for the alkali atoms; ii) the mass ratio plays an important role in the energy exchange between the two species and, as shown below, the parallel temperature of the seeded gas (mass m_2) is considerably lower than the parallel temperature of the carrier gas (mass m_1) when $m_2 \ll m_1$.

The main goal of the present paper is to present a detailed derivation of our theoretical analysis of this effect. We first recall the calculation of the terminal parallel temperature in a pure gas expansion, discussing the various approximations. Then, we generalize this calculation to the case of a gas mixture, in the limit of a high dilution and we describe in detail our approximations. In the final part, we present a set of experiments made with a beam of lithium seeded in argon.

II. TERMINAL PARALLEL TEMPERATURE IN SUPERSONIC EXPANSION OF A PURE MONOATOMIC GAS

In a first step, we follow here the detailed analysis developed by Toennies and Winkelmann [4] (noted below TW) in 1977, with emphasis on the special case of helium expansion. Then, we use the approximations introduced by Beijerinck and Verster [5] in 1981 (noted below BV) to simplify the calculations. Thanks to these approximations, BV were able to demonstrate analytically a scaling law for the terminal value of the parallel speed ratio.

A. Equations describing the cooling effect during a supersonic expansion

To describe the cooling effect in a supersonic expansion, we must start from the Boltzmann equation:

$$\mathbf{v} \cdot \mathbf{grad}\left[n(\mathbf{r}) f(\mathbf{r}, \mathbf{v})\right] = \left(\frac{\partial (nf)}{\partial t}\right)_{coll} \tag{1}$$

We have assumed a steady state regime and we have split the phase space particle density as the product of the density in space $n(\mathbf{r})$ by a normalized velocity distribution $f(\mathbf{r}, \mathbf{v})$. Following TW, the geometry of a supersonic expansion seems impossible to handle in a fully analytic treatment and near its axis, the expansion is approximated by a spherically symmetric flow. The solution of the Boltzmann equation is then made by the method of moments. In this method, the first step is to assume that the velocity distribution remains Maxwellian, but with different parallel and perpendicular temperatures $T_\parallel$ and $T_\perp$:

$$f(\mathbf{r}, \mathbf{v}) = \left(\frac{m}{2\pi k_B T_\parallel}\right)^{1/2} \times \frac{m}{2\pi k_B T_\perp} \exp\left[-\frac{m\left(v_\parallel - u\right)^2}{2k_B T_\parallel} - \frac{m v_\perp^2}{2k_B T_\perp}\right] \tag{2}$$

where m is the atomic mass and u is the local hydrodynamic velocity. Using spherical coordinates r, θ and ϕ, the Boltzmann equation becomes:

$$v_\parallel \frac{\partial f}{\partial r} - \frac{m}{r k_B T_\parallel}\left(v_\parallel - u\right) v_\perp^2 f + \frac{m}{r k_B T_\perp} v_\parallel v_\perp^2 f = \left(\frac{\partial f}{\partial t}\right)_{coll} \tag{3}$$

The second step of the method of moments consists in integrating the Boltzmann equation multiplied by some quantity χ. Using successively $\chi = 1$, $\chi = v_\parallel$, $\chi = v_\parallel^2 + v_\perp^2$, $\chi = v_\perp^2$, TW obtained differential equations coupling the density n, the hydrodynamic velocity u and the temperatures $T_\parallel$ and $T_\perp$:

$$\frac{d\left(nur^2\right)}{dr} = 0 \tag{4}$$

$$nu\frac{du}{dr} + \frac{d}{dr}\left(\frac{nk_B T_\parallel}{m}\right) + \frac{2nk_B\left(T_\parallel - T_\perp\right)}{mr} = 0 \tag{5}$$

$$\frac{d}{dr}\left(u^2 + \frac{3k_B T_\parallel}{m} + \frac{2k_B T_\perp}{m}\right) = 0 \tag{6}$$

$$\frac{dT_\perp}{dr} + \frac{2T_\perp}{r} = \mathcal{F} \tag{7}$$

Equation (4) has been used to simplify equations (5,6,7). The collision term $\mathcal{F}$ in equation (7) is discussed below. Equation (4) expresses the conservation of atom flux and will be used to relate the density n to the distance r. After integration, equation (6), which expresses energy conservation, takes the following form:

$$u = \sqrt{k_B\left(5T_0 - 3T_\parallel - 2T_\perp\right)/m} \tag{8}$$

After some algebra, we get the equation giving the variations of the parallel temperature:

$$\frac{dT_\parallel}{dr} = -\left[\frac{4T_\perp}{r} \times \frac{k_B T_\parallel}{mu^2} + 2\left(1 - \frac{k_B T_\parallel}{mu^2}\right)\mathcal{F}\right] / \left[1 - \frac{3k_B T_\parallel}{mu^2}\right] \tag{9}$$

Introducing the parallel speed ratio $S_\parallel = u/\sqrt{2kT_\parallel/m}$, we can express the ratio $k_B T_\parallel/(mu^2)$ which appears in equation (9) as equal to $1/(2S_\parallel^2)$. In most supersonic expansions, $S_\parallel$

becomes large so that the terms involving $k_B T_\parallel/(mu^2)$ can be neglected. We thus get two coupled differential equations giving the variations of the parallel and perpendicular temperatures:

$$\frac{dT_\parallel}{dr} = -2\mathcal{F} \tag{10}$$

$$\frac{dT_\perp}{dr} = -\frac{2T_\perp}{r} + \mathcal{F} \tag{11}$$

These equations have an interesting form: the cooling effect comes from the geometrical cooling effect (see figure 1 of TW) acting only on the perpendicular degrees of freedom, which is expressed by the $-2T_\perp/r$ term. The geometrical cooling effect is transferred to the parallel degree of freedom through the collision term $\mathcal{F}$ given by:

$$\mathcal{F} = \frac{n}{2k_B u}\int g\frac{d\sigma(g)}{d\Omega}\Delta E f(\mathbf{v}_1) f(\mathbf{v}_2) d^3\mathbf{v}_1 d^3\mathbf{v}_2 d\Omega \tag{12}$$

$\mathbf{v}_1$ and $\mathbf{v}_2$ are the velocities of the two atoms before the collision and $\mathbf{g} = \mathbf{v}_1 - \mathbf{v}_2$ is their relative velocity of modulus g, while $d\sigma(g)/d\Omega$ is the collision differential cross-section. ΔE is the energy transferred during one collision from the parallel degree of freedom to the perpendicular ones for the two atoms. After averaging over the azimuth φ describing the direction of the final relative velocity around the initial relative velocity, ΔE is given by :

$$\langle \Delta E \rangle_\varphi = \frac{m}{8}\left[g_\perp^2 - 2g_\parallel^2\right]\left[1 - \cos^2\chi\right] \tag{13}$$

where χ is the deflection angle.

B. Simplification of these equations

BV have shown that the coupling term $\mathcal{F}$ is well approximated by a linear function of $(T_\parallel - T_\perp)$. This approximation appears to be good and it leads to simple coupled equations for the parallel and perpendicular temperatures:

$$\mathcal{F} \approx \Lambda(z)\left(T_\parallel - T_\perp\right) \text{ with } \Lambda(z) = 16 n(z)\Omega^{(2,2)}(T_m)/(15u_\infty) \tag{14}$$

From now on, we follow BV in noting $z = r$ the distance from the nozzle. $\Omega^{(l,s)}(T)$ is a thermal average of the collision integral $Q^{(l)}$, both defined in Appendix A. $T_m = (T_\parallel + 2T_\perp)/3$ is the weighted mean of the parallel and perpendicular temperatures. Finally, the hydrodynamic velocity u, which appears in equation (12), has been approximated by its terminal value u_∞, given by $u_\infty = \sqrt{5k_B T_0/m}$ in the large $S_{\parallel\infty}$ limit. Neglecting quantum effects, if the interaction potential is approximated by a 12-6 Lennard-Jones potential, the $\Omega^{(2,2)}(T)$ integral is given by:

$$\Omega^{(2,2)}(T) = 2.99\left(\frac{2k_B T}{m}\right)^{1/2}\left(\frac{C_6}{k_B T}\right)^{1/3} \tag{15}$$

where C_6 is the coefficient of the attractive term of the potential. This formula has been established by BV, assuming that the relative kinetic energy is small with respect to the

interaction potential well depth ϵ. The validity range of this equation is discussed in Appendix A. Finally, we need the value of $n(z)$ which is given by equation (16) and can be related to the source density n_0 and temperature T_0. We will use the approximate formula:

$$n(z) \approx I/(u_\infty z^2) \tag{16}$$

where I is the intensity of the supersonic beam. This quantity is usually evaluated by solving the continuum equations of supersonic flow in the vicinity of the nozzle (see BV for a derivation of this result):

$$I = n_0 u_\infty z_{ref}^2 \tag{17}$$

with $z_{ref} = 0.403 \times d$, where d is the nozzle diameter. We thus get two coupled equations giving the parallel and perpendicular temperatures:

$$\frac{dT_\parallel}{dz} = -\Lambda(z)\left(T_\parallel - T_\perp\right) \tag{18}$$

$$\frac{dT_\perp}{dz} = -\frac{2T_\perp}{z} + \frac{\Lambda(z)}{2}\left(T_\parallel - T_\perp\right) \tag{19}$$

with $\Lambda(z)$ given by:

$$\Lambda(z) = 3.189 \times \frac{n_0 z_{ref}^2}{u_\infty z^2}\left(\frac{2k_B T_m}{m}\right)^{1/2}\left(\frac{C_6}{k_B T_m}\right)^{1/3} \tag{20}$$

$\Lambda(z)$ is proportional to $T_m^{1/6} z^{-2}$.

C. Scaling and integration of these equations

In the beginning of the expansion, the density is large and the collision term $\mathcal{F}$ is large enough to keep the two temperatures equal, $T_\parallel = T_\perp = T_m$. Then, the mean temperature T_m verifies:

$$\frac{dT_m}{dz} = -\frac{4T_m}{3z} \tag{21}$$

which leads to:

$$T_m \propto z^{-4/3} \tag{22}$$

This behavior agrees with the prediction of continuum equations. To study the equations (18,19) in the general case, we make a first scaling introduced by BV, with reduced temperatures (obtained by dividing the temperatures $T_\parallel$, $T_\perp$, T_m by T_0) and a reduced distance $z_r = z/z_{ref}$:

$$\frac{dT_{\parallel r}}{dz_r} = -\Xi\frac{T_{mr}^{1/6}}{z_r^2}\left(T_{\parallel r} - T_{\perp r}\right) \tag{23}$$

$$\frac{dT_{\perp r}}{dz_r} = -\frac{2T_{\perp r}}{z_r} + \Xi\frac{T_{mr}^{1/6}}{2z_r^2}\left(T_{\parallel r} - T_{\perp 1,r}\right) \tag{24}$$

All the source parameters are condensed in the quantity $\Xi = 0.814 \times n_0 d \left(C_6/k_B T_0\right)^{1/3}$, which is dimensionless. Following BV, a further scaling can be made to eliminate Ξ from these equations:

$$z_r = \zeta \Xi^{9/11} \text{ and } T_{Xr} = \tau_X \Xi^{-12/11} \tag{25}$$

with $X = \parallel$ or $\perp$. The exponents of Ξ are easily determined by eliminating Ξ from equations (23, 24) but we must also consider an equation deduced from equation (22). This scaling provides the following universal equations:

$$\frac{d\tau_\perp}{d\zeta} = -\frac{2\tau_\perp}{\zeta} + \frac{\tau_m^{1/6}(\tau_\parallel - \tau_\perp)}{2\zeta^2} \tag{26}$$

$$\frac{d\tau_\parallel}{d\zeta} = -\frac{\tau_m^{1/6}(\tau_\parallel - \tau_\perp)}{\zeta^2} \tag{27}$$

These equations have been integrated numerically by BV and it is easy to reproduce their calculation (see below figure 1). An important result is the terminal value of $\tau_\parallel$, $\tau_{\parallel\infty} = 1.15$, from which we deduce the final perpendicular temperature as a function of source parameters:

$$T_{\parallel\infty}/T_0 = 1.15 \times \Xi^{-12/11} \tag{28}$$

D. Results, discussion and tests in the case of argon expansion

The tradition is to give the terminal value $S_{\parallel\infty}$ of the parallel speed ratio rather than the terminal parallel temperature $T_{\parallel\infty}$. For completeness, let us recall the relation in the case of a monoatomic gas:

$$T_{\parallel\infty} = T_0 / \left(1 + 0.4 S_{\parallel\infty}^2\right) \tag{29}$$

The theoretical results of TW and BV have the same form and we have written them in SI units so that they can be compared:

$$S_{\parallel\infty} = A \left[n_0 d \left(C_6/k_B T_0\right)^{1/3}\right]^\delta \tag{30}$$

The values of A and δ obtained by TW are $A = 1.413$ and $\delta = 0.53$, resulting from a fit to the data obtained by numerical integration of the equations established in part II.A without approximations. BV obtained $A = 1.313$ and $\delta = 0.545$. In the range of practical interest, when $5 < S_{\parallel\infty} < 50$, these two formula never differ by more than 4% and agree for $S_{\parallel\infty} \approx 18.9$.

Let us discuss the validity of these theoretical results:

- a basic assumption is the use of the methods of moments, which assumes that the velocity distribution remains Maxwellian, with different parallel and perpendicular temperatures. As discussed by BV, this assumption is not excellent: at the end of the expansion, when collisions become rare and when the two temperatures are very different, the velocity distribution for the perpendicular degrees of freedom differs from a Maxwellian distribution. However, the excellent description of helium expansions

by TW proves that the use of this method is a good approximation, at least for the calculation of the parallel temperature.

- with respect to the TW calculations, the BV treatment makes several further approximations, in particular the linearization expressed by equation (14). The consequences of these approximations on the results are very minor, as shown by the good agreement between the TW and BV results.

- in both calculations, the temperature dependence of the $\Omega^{(2,s)}$ integral is the same, relying on a scaling law of the cross-section in $(C_6/k_BT)^{1/3}$. As pointed out by Miller [8], the cross-section is thus underestimated in the initial part of the expansion, when T_0 is large. Fortunately, as shown above, in the beginning of the expansion, the collision term $\mathcal{F}$ is very large and its exact value has no importance as long as it is sufficient to maintain $T_\parallel = T_\perp$. It is only when the collisions become rare, i.e. when the two temperatures start to differ that the exact value of the collision integral $\Omega^{(2,s)}$ is important. Fortunately, this occurs when the parallel temperature reaches 2 or 3 times its final value, well in the range where the scaling law (15) is expected to be good, as discussed in Appendix A.

- the mathematical form of equation (30) is probably at the origin of a misunderstanding concerning the terminal value of the speed ratio. In fact, this misunderstanding dates back from earlier works [2, 3] which expressed the terminal value of the speed ratio as a function of the Knudsen number calculated at the nozzle. This form suggests that the terminal speed ratio will increase with the mean number of collisions during the expansion. This is not true if the cross-section depends rapidly on the temperature: if one could increase the collision rate near the source temperature without modifying its value at low temperatures, the total number of collisions will be changed but the terminal speed ratio will not be modified.

BV made also a fit of experimental $S_{\parallel\infty}$ values for argon expansions. In such a fit, BV have corrected the nozzle diameter d for the boundary layer and this correction is not negligible. Using $C_6(Ar - Ar)/k_B = 4.45 \times 10^{-55}$ K.m^6, they obtained $A = 1.782$ and $\delta = 0.495$. We insist on the C_6 value used, which is very close to the best evaluations of this coefficient, because some authors use an effective value deduced from the core-radius σ and the potential well depth ϵ using the relation $C_6 = 4\epsilon\sigma^6$ valid for Lennard-Jones 12-6 potential (see for example, Miller [8]) and such a value is roughly twice as large. The semi-empirical law of BV has been compared by Beijerinck, Manger and Verster [9] with the 1969 data of Miller and Andres [10], the measured speed ratio being clearly lower than the prediction of the semi-empirical law. The difference may be probably explained by the interaction with the residual gas and with the skimmer, as discussed by Buck et al. [11]. We have also compared this semi-empirical law with measurements made by H. D. Meyer [12]. From this comparison which is quite satisfactory (except for large values of the source pressure, near the onset of condensation in the beam), we think that the semi-empirical law of BV is accurate and we estimate its error bar near $\pm 7\%$.

III. GENERALIZATION TO THE CASE OF A MIXTURE OF TWO MONOATOMIC GASES

We follow exactly the same derivation as in the previous part. This generalization is straightforward but the equations are more complex and an analytic solution requires some further approximations.

A. Approximations used to solve the Boltzmann equation

Still starting from the Boltzmann equation, we have now two equations, one per species noted $i = 1$ for the carrier gas and $i = 2$ for the seeded gas:

$$\mathbf{v}_i \cdot \mathbf{grad}\left[n_i(\mathbf{r}) f_i(\mathbf{r}, \mathbf{v}_i)\right] = \Sigma_{j=1,2} \left(\frac{\partial\left(n_i f_i\right)}{\partial t}\right)_{coll} (i, j) \tag{31}$$

The collision terms have now two parts corresponding to the two possible types of collision pairs. The densities $f_i(\mathbf{r}, \mathbf{v}_i)$ are expressed by equation (2), with the atomic masses m_i, the temperatures $T_{\parallel i}$ and $T_{\perp i}$.

We make the approximation that the hydrodynamic velocity u is the same for both species. This approximation is poor when a very heavy species is seeded in a light gas, because many collisions are needed to accelerate the heavy species. Here, we are mostly interested by the opposite case, with a light atom seeded in a heavy carrier gas. If the expansion is well in the supersonic regime, the difference of the mean velocities is expected to be very small and the rms parallel velocities will be considerably larger than this small difference. We will prove the validity of this approximation below.

A second approximation is to consider only the case of high dilution, i.e. that the seeded gas density n_2 is considerably smaller than the carrier gas density n_1. This assumption greatly simplifies the calculations and the experiments discussed in part IV are well in this regime. Because $n_2 \ll n_1$, in the Boltzmann equation for the carrier gas distribution function f_1, we can neglect the $1-2$ collision term and this simply means that, with an excellent approximation, the expansion of the carrier gas is not modified by the presence of the seeded gas. Therefore, the equations written above can be used to calculate its parallel and perpendicular temperatures now noted $T_{\parallel 1}$ and $T_{\perp 1}$, by introducing in $\Lambda(z)$ the relevant collision integral $\Omega_{1,1}^{(2,2)}(T)$ where the indices designate the colliding atom pair.

In the Boltzmann equation for the seeded gas distribution function f_2, it is an excellent approximation to consider only the effect of $1-2$ collisions, i.e. collisions with atoms of the carrier gas and to neglect the collisions involving two atoms of the seeded species 2, because they are considerably less numerous. Then, using the same procedure and the same approximations done above, we get the following equations for the temperatures describing the seeded species:

$$\frac{dT_{\parallel 2}}{dr} = 2\mathcal{F}_{\parallel,2} \tag{32}$$

$$\frac{dT_{\perp 2}}{dr} = -\frac{2T_{\perp 2}}{r} + \mathcal{F}_{\perp 2} \tag{33}$$

with the collisional energy transfer terms given by:

$$\mathcal{F}_{X,2} = \frac{n_1}{k_B u} \int g \frac{d\sigma_{1,2}(g)}{d\Omega} \Delta E_{X,2} f_1(\mathbf{v}_1) f_2(\mathbf{v}_2) d^3\mathbf{v}_1 d^3\mathbf{v}_2 d\Omega \tag{34}$$

where $\Delta E_{X,2}$ ($X = \parallel$ or $\perp$) measures the parallel or perpendicular energy gained by atom 2 during the collision with atom 1. With respect to equation (12), there are several interesting differences:

- a factor 2 in the denominator of equation (34) is missing because the number of $1-2$ collisions is proportional to $n_1 n_2$ while the number of $1-1$ collisions is proportional to $n_1^2/2$.
- an obvious consequence of energy conservation makes that, in the pure gas case, all the energy lost by the parallel degree of freedom appears in the perpendicular degrees of freedom. Now, the initial energy is shared after the collision between the atoms 1 and 2 and this simple relation does not exist anymore. We can express $\Delta E_{X,2}$ with the parallel and perpendicular components of the center of mass velocity and of the relative velocity. However, when the four temperatures ($T_{\parallel i}$ and $T_{\perp i}$ with $i = 1, 2$) are not equal, the product $f_1(\mathbf{v}_1) f_2(\mathbf{v}_2)$ does not take a simple form when expressed with the center of mass velocity and the relative velocity and we have not found how to calculate exactly the resulting integrals.
- therefore, an analytic calculation of $\mathcal{F}_{X,2}$ requires some new approximations. The cross-sections $Q^{(l)}_{1,2}(g)$ behave like $g^{-2/3}$ when the energy of the relative motion $E = \mu g^2/2$ ($\mu = m_1 m_2/(m_1+m_2)$ being the reduced mass) is small ($E \ll \epsilon(1-2)$, the well depth of the $1-2$ interaction potential). Therefore, the products $g Q^{(l)}_{1,2}(g)$ vary slowly with g, like $g^{1/3}$. We take the quantity $g d\sigma_{1,2}(g)/d\Omega$ out of the integrals over $\mathbf{v}_1$ and $\mathbf{v}_2$, which are thus considerably simplified:

$$\mathcal{F}_{X,2} \approx \frac{n_1}{k_B u_\infty} \int \langle g \frac{d\sigma_{1,2}(g)}{d\Omega} \rangle d\Omega \int \Delta E_{X,2} f_1(\mathbf{v}_1) f_2(\mathbf{v}_2) d^3\mathbf{v}_1 d^3\mathbf{v}_2 \tag{35}$$

  This calculation is described in appendix B.

B. Coupled equations describing the temperatures of the two gases

The coupled equations for the carrier gas $i = 1$ are simply the equations established in part II , equations (18) and (19) where T_X is replaced by T_{X1}. In the differential equations for the temperatures of the seeded gas $i = 2$, we have quantities similar to $\Lambda(z)$ but involving the $\Omega^{(l,2)}_{1,2}(T_m)$ integrals with $l = 1$ and 2. By introducing two dimensionless ratios ρ_s and ρ_o, we can express these quantities as a function of $\Omega^{(2,2)}_{1,1}(T_m)$. ρ_s is the ratio of $\Omega^{(2,2)}_{i,j}$ collision integrals differing by the species of the second collision partner and its value is deduced from equation (15):

$$\rho_s = \frac{\Omega^{(2,2)}_{1,2}}{\Omega^{(2,2)}_{1,1}} = \left[\frac{C_6(1,2)}{C_6(1,1)}\right]^{1/3} \times \left[\frac{m_1+m_2}{2m_2}\right]^{1/2} \tag{36}$$

ρ_s depends slowly on the C_6 ratio and more rapidly on the mass ratio. ρ_o is the ratio of angle-averaged cross-sections of orders $l = 1$ and $l = 2$:

$$\rho_o = \frac{Q_{1,2}^{(1)}}{Q_{1,2}^{(2)}} = \frac{\Omega_{1,2}^{(1,2)}}{\Omega_{1,2}^{(2,2)}} \tag{37}$$

In our previous paper [1], we have used $\rho_o = 1.32$ (see also Appendix A).

$$\begin{aligned} \frac{dT_{\perp 2}}{dz} &= -\frac{2T_{\perp 2}}{z} + \Lambda(z)\rho_s \frac{m_1}{M}\left[T_{\parallel,av} - T_{\perp,av}\right] \\ &- 4\Lambda(z)\rho_s\rho_o \frac{\mu}{M}\left[T_{\perp 2} - T_{\perp 1}\right] \end{aligned} \tag{38}$$

$$\begin{aligned} \frac{dT_{\parallel 2}}{dz} &= -2\Lambda(z)\rho_s \frac{m_1}{M}\left[T_{\parallel,av} - T_{\perp,av}\right] \\ &- 4\Lambda(z)\rho_s\rho_o \frac{\mu}{M}\left[T_{\parallel 2} - T_{\parallel 1}\right] \end{aligned} \tag{39}$$

$\Lambda(z)$ being given by equation (20) and $T_{X,av}$ ($X = \parallel$ or $\perp$) being defined by:

$$T_{X,av} = \beta T_{X1} + \alpha T_{X2} \tag{40}$$

$$\alpha = m_1/M \ , \ \beta = m_2/M \text{ and } M = m_1 + m_2 \tag{41}$$

One must remark that in $T_{X,av}$, the weight of T_{X1} is $\beta = m_2/M$ and the weight of T_{X2} is $\alpha = m_1/M$. As in part I.C, we introduce reduced temperatures and a reduced z-coordinate, by dividing the temperatures by T_0 and the distance z by z_{ref} and we then eliminate Ξ by introducing τ and ζ. We thus get the following equations for $\tau_{\parallel 2}$ and $\tau_{\perp 2}$:

$$\begin{aligned} \frac{d\tau_{\perp 2}}{d\zeta} &= -\frac{2\tau_{\perp 2}}{\zeta} + \frac{\rho_s \tau_m^{1/6}}{\zeta^2} \times \frac{m_1}{M}\left(\tau_{\parallel,av} - \tau_{\perp,av}\right) \\ &- \frac{4\rho_s\rho_o\tau_m^{1/6}}{\zeta^2} \times \frac{\mu}{M}\left(\tau_{\perp 2} - \tau_{\perp 1}\right) \end{aligned} \tag{42}$$

$$\begin{aligned} \frac{d\tau_{\parallel 2}}{d\zeta} &= -\frac{2\rho_s \tau_m^{1/6}}{\zeta^2} \times \frac{m_1}{M}\left(\tau_{\parallel,av} - \tau_{\perp,av}\right) \\ &- \frac{4\rho_s\rho_o\tau_m^{1/6}}{\zeta^2} \times \frac{\mu}{M}\left(\tau_{\parallel 2} - \tau_{\parallel 1}\right) \end{aligned} \tag{43}$$

We do not reproduce the equations (26,27) verified by $\tau_{\parallel 1}$ and $\tau_{\perp 1}$.

As we have done several approximations and as the calculations are rather involved, it is interesting to test their coherence. If we assume that the two species have the same masses ($m_1 = m_2$) and the same collision cross-sections ($\rho_s = 1$), we expect that the parallel and perpendicular temperatures are independent of the species at all time. It is easy to derive the equations for the differences $(\tau_{X1} - \tau_{X2})$ with $X = \parallel$ or $\perp$ and to verify that if these differences are initially equal to zero, they remain equal to zero. Direct numerical integration

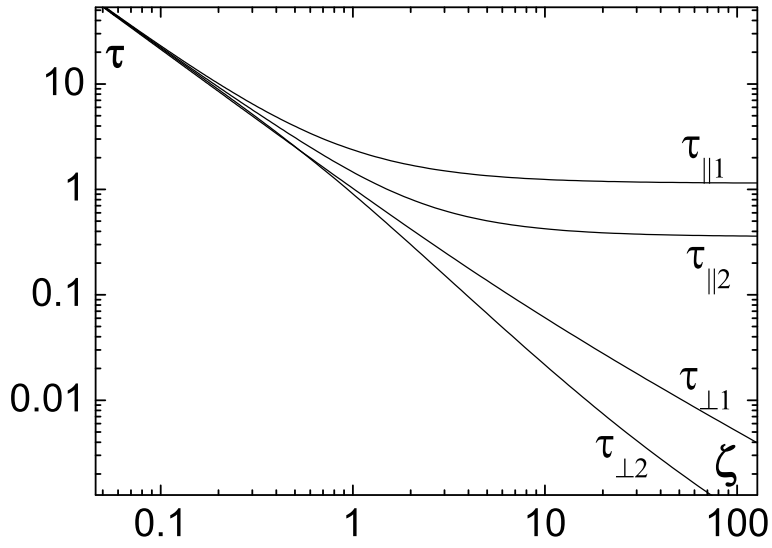

FIG. 1: The reduced temperatures $\tau = \Xi^{-9/11} T/T_0$ are plotted as a function of the reduced z-coordinate $\zeta = 2.48\Xi^{12/11} z/d$ with $\Xi = 0.813 n_0 d\,(C_6/k_B T_0)^{1/3}$. For $\tau_{\|1}$ and $\tau_{\perp 1}$, this plot is identical to figure 5 of Beijerinck and Verster [5] and the results for $\tau_{\|2}$ show the anomalous cooling effect. The calculation is made with $\rho_s = 2.55$ corresponding to the case of lithium seeded in argon and with $\rho_o = 1.32$.

of the coupled equations supports this idea, although we observe a small difference on the terminal values of parallel temperatures, $\tau_{\|2}$ being 5% lower than τ_{X1} (this weak difference is probably due to numerical instabilities).

Numerical integration of equations (42,43) provides the temperatures represented in figure 1. At the end of the expansion, the parallel and perpendicular temperatures of the seeded gas are lower than the similar quantities for the carrier gas. In particular, the terminal value of the parallel temperature ratio $\tau_{\|2,\infty}/\tau_{\|1,\infty} = T_{\|2,\infty}/T_{\|1,\infty}$ can be substantially lower than 1. The absolute minimum value for this temperature ratio is reached when the right-hand side of equation (39) vanishes. Assuming that the perpendicular temperatures are both negligible, we get the minimum possible value of the ratio $T_{\|2,\infty}/T_{\|1,\infty}$:

$$\mathrm{Min}\left(\frac{T_{\|2,\infty}}{T_{\|1,\infty}}\right) = \frac{m_2 \rho_o}{m_1 + 2 m_2 \rho_o} \tag{44}$$

This limiting value would be reached if the number of $1-2$ collisions is sufficiently larger than the number of $1-1$ collisions, i.e. if the ratio ρ_s is sufficiently large. We have plotted in figure 2 the terminal value of the ratio $T_{\|2,\infty}/T_{\|1,\infty}$ for various values of the ratio ρ_s and for different values of the mass ratio m_2/m_1. The anomalous cooling effect can be quite large, when the mass ratio m_2/m_1 is very small. We predict a particularly large effect in the case of molecular hydrogen H_2 seeded in argon. Usually, molecular hydrogen behaves almost like an atom in supersonic expansion, because relaxation of molecular rotation is very slow in

this case. We have calculated the Ar-H_2 C_6 coefficient with the combination rule and data of Kramer and Herschbach [13]. We thus get $\rho_s = 2.48$ from which we calculate a temperature ratio $T_{\|2,\infty}/T_{\|1,\infty} = 0.164$, which should be easy to observe.

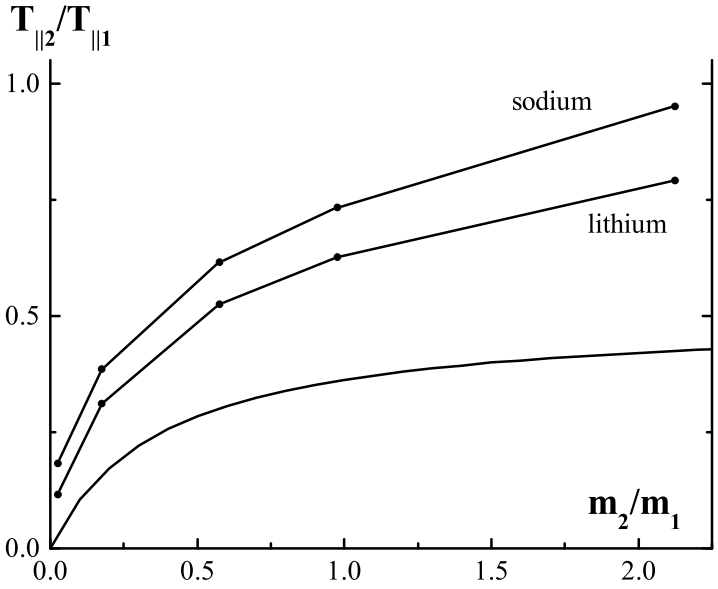

FIG. 2: The calculated parallel temperature ratio $T_{\|2\infty}/T_{\|1\infty}$ is plotted as a function of the mass ratio m_2/m_1, spanning the range from hydrogen to rubidium seeded in argon, for several values of the ratio ρ_s, with ρ_o fixed, $\rho_o = 1.32$. From bottom to top, $\rho_s = \infty$, $\rho_s = 1.67$ (corresponding to sodium seeded in argon), $\rho_s = 2.55$ (corresponding to lithium seeded in argon).

C. Discussion

We may discuss the validity of our derivation. In addition to the approximations already done by Beijerinck and Verster, we have introduced several new approximations:

- we have assumed the same hydrodynamic velocity for the two species i.e. we have neglected the velocity slip, which has been studied by Anderson [6] and by Miller and Andres [10]. Using the equations (2.37,2.38) of the review paper written by Miller [8]), we can express the velocity difference $u_{2,\infty} - u_{1,\infty}$ with our notations:

$$\frac{u_{2,\infty} - u_{1,\infty}}{u_{1,\infty}} \approx 0.59 \left[\frac{\sqrt{\mu m_1}}{|m_1 - m_2|} n_0 d \left(C_6 / k_B T_0 \right)^{1/3} \right]^{-1.07} \tag{45}$$

  In appendix A, we have evaluated the $\Omega_{1,2}^{(1,1)}$ integral, which appears in equations (2.37,2.38) of reference [8]. We have replaced the mole fraction average mass by its value m_1 in the high dilution limit. The physically important quantity is the ratio

of this velocity difference $(u_{2,\infty} - u_{1,\infty})$ divided by the terminal parallel thermal velocity of atom 1, namely $\sqrt{2k_B T_{\parallel 1}/m_1}$. Using equation (30) in the TW form and approximating the 1.07 exponent by 2×0.53, we get:

$$\frac{u_{2,\infty} - u_{1,\infty}}{\sqrt{2k_B T_{\parallel 1}/m_1}} \approx \frac{0.84}{S_{\parallel 1\infty}} \left[\frac{(m_1 + m_2)(m_1 - m_2)^2}{m_1^2 m_2} \right]^{0.53} \tag{46}$$

In this form, it is clear that, if the terminal parallel speed ratio $S_{\parallel 1\infty}$ is large, the velocity slip is a small fraction of the parallel thermal velocity of atom 1, provided that the masses m_1 and m_2 are not extremely different. In this case, our approximation is very good.

- we have done the calculation in the high dilution limit: this is not an approximation but the general case would be interesting to study, for practical applications.

- we have treated the products $gQ_{1,2}^{(l)}(g)$ as constant, in order to be able to handle the averages of the transferred energy over the elliptic velocity distributions. Takahashi and Teshima were able to calculate numerically these integrals when they studied the case of a heavy gas seeded in a light gas [14]. Using the same technique, it would be possible to test the accuracy of our approximation.

In conclusion, we believe that our approximations are valid and accurate. Numerical simulation can provide further support to our analytic results. Following P. Skovorodko [15], several methods can be used to simulate flows of gases and gas mixtures: the Direct Simulation Monte Carlo method described by G. A. Bird [16] is the best method but it requires much computation in the high dilution case. P. Skovorodko has used the Test Particle Monte Carlo method to simulate the expansion of gas mixtures; for computational needs, this method involves other approximations, in particular the use of Maxwell type interaction potential. He was able to simulate our lithium seeded in argon expansion and his results support our calculations, at least at the qualitative level [17].

IV. COMPARISON WITH EXPERIMENTAL RESULTS

Here, we compare our theoretical results with a new set of experiments made on a supersonic beam of lithium seeded in argon.

A. Our lithium beam

Our beam [18] is largely inspired by the design used by Broyer, Dugourd and coworkers to produce lithium clusters [19]. As we need a lithium pressure of the order of 1 millibar only, we have used Thermocoax heating elements instead of radiative heating. Our oven is surrounded by two thermal shields, to save heating power, and by a water-cooled copper shield, to prevent excessive heating of the vacuum tank. The temperatures used in our experiment are usually equal to 973 K for the back part, corresponding to a lithium vapor pressure of 0.55 millibar and to 1073 K for the front part. The nozzle is a hole of 200 μm diameter drilled in a stainless steel 0.3 mm thick wall. The argon gas (from Air Liquide, 99.999 % stated purity) is further purified by a purifying cartridge also from Air Liquide.

The argon pressure can be varied from 150 to 800 millibar. The upper value is limited by the pumping speed of our pumping system made of a Varian VHS400 oil diffusion pump (8000 l/s pumping speed) backed by a Leybold D65B roughing pump (65 m^3/hour pumping speed). For a source pressure $p_0 = 300$ millibar, the pressure measured near the VHS400 pump is 8×10^{-4} millibar. We use a skimmer provided by Beam Dynamics; its position is fixed, while the oven position can be adjusted under vacuum, the nozzle to skimmer distance being 20 mm. After the skimmer, the lithium beam is in a separate vacuum tank pumped by a Varian VHS6 oil diffusion pump (2400 l/s pumping speed) fitted with a water cooled baffle. Under beam operation, when $p_0 = 300$ millibar, the pressure in this chamber is 6×10^{-6} millibar so that the interaction of the beam with the residual gas should not be very large.

B. Doppler measurement of the parallel and perpendicular velocity distribution

In the center of the second vacuum tank i.e. 225 mm after the skimmer, the lithium beam is crossed by two laser beams A and B. The angle between the atomic beam and the laser beams are $\theta_A = 47.9 \pm 0.5°$ and $\theta_B \approx 90°$.

The first order Doppler effect is sensitive only to the projection v_p of the velocity on the laser beam axis. For a laser beam making the angle θ with the axis of the atomic beam, the distribution of v_p is deduced from equation (2):

$$f(v_p) = \left(\frac{m}{2\pi k_B T(\theta)}\right)^{1/2} \exp\left[-\frac{m\,(v_p - u\cos\theta)^2}{2k_B T(\theta)}\right] \tag{47}$$

with:

$$T(\theta) = T_\parallel \cos^2\theta + T_\perp \sin^2\theta \tag{48}$$

The distribution $f(v_p)$ is centered at $v_p = u\cos\theta$ and its width is characterized by a weighted mean of the parallel and perpendicular temperatures. The fluorescence intensity as a function of the laser frequency reflects very accurately the velocity distribution if two conditions are fulfilled:

- the natural width of the excited transition is negligible with respect to the Doppler width
- saturation broadening of the transition as well as laser frequency jitter are both negligible.

Our laser excites the hyperfine components of the $^2S_{1/2}$ - $^2P_{3/2}$ resonance transition of lithium at 671 nm [20]. The very small hyperfine splittings of the upper state can be neglected. The ground state has two hyperfine components $F = 1$ and $F = 2$, with a splitting equal to 803.5 MHz. The natural width of the transition is $\Gamma/2\pi = 5.87$ MHz [21] and we use laser power density of the order of 10^{-2} mW/cm^2, corresponding to a saturation parameter $s \approx 5 \times 10^{-3}$ and a negligible broadening of the excitation line. The laser used is a single frequency cw dye laser pumped by a Spectra-Physics argon ion laser, the dye being LD 688 from Exciton dissolved in EPH. Using the Hänsch-Couillaud [22] frequency stabilization technique, we get a laser linewidth of the order of 1 MHz.

We have recorded a series of laser induced fluorescence spectra for different argon pressures in the beam source. Figure 3 shows such a spectrum. The observed Doppler widths fall in the

$90 - 120$ MHz range, for beam B, which is sensitive to the parallel velocity distribution: the natural width as well as the laser linewidth are clearly negligible. During our experiment, we have also recorded a saturated absorption spectrum in a heat pipe oven: this signal provides Doppler-free peaks which are useful if one wants to measure accurately the mean velocity u of the atomic beam, because, in some experiments, the laser beam B is not exactly perpendicular to the atomic beam.

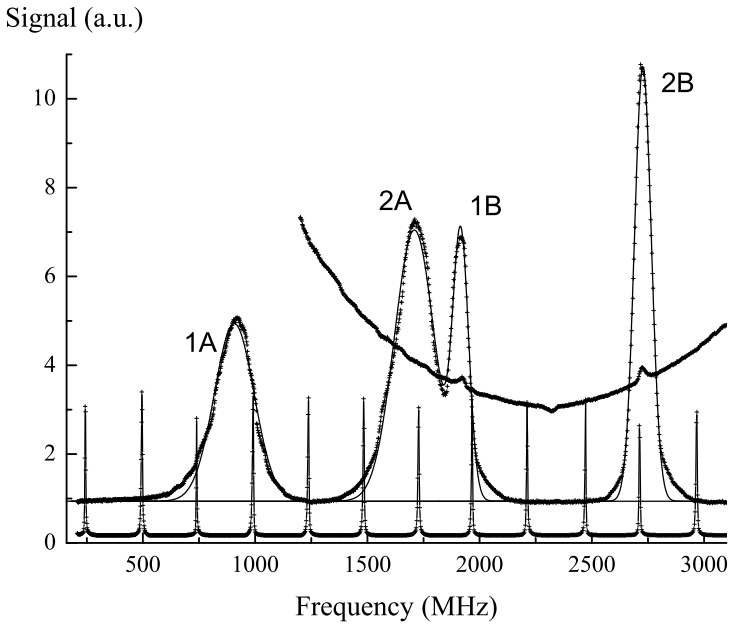

FIG. 3: Laser induced fluorescence signal as a function of the laser frequency: the dots represent the experimental data and the full curves are the Gaussian fits to each line. The Fabry-Perot used for calibration has a free spectral range equal to 251.4 ± 0.5 MHz. The saturated absorption spectrum providing lithium Doppler-free peaks is represented for frequencies above 1250 MHz. The fluorescence peaks are labeled by the ground state F value ($F = 1$ or 2) and by a letter corresponding to the laser beam. The angle between the atomic beam and the laser beam is $\theta_A = 47.9 \pm 0.5^\circ$ for beam A and $\theta_B \approx 90^\circ$ for beam B.

C. Experimental results

The analysis of a fluorescence spectrum provides various information collected in table IV C for various sources pressures. From the distance between the A and B peaks, we can deduce the beam mean velocity u. The measured values are close to $u = 1010 \pm 10$ m/s, slightly less than the value deduced from the source temperature, $u_\infty = \sqrt{5k_BT_0/m} = 1056$ m/s. The width of the B peak is related to the perpendicular temperature of the beam: we think that the perpendicular temperature $T_\perp$ thus deduced is overestimated because our detector is not observing only one streamline. The width of the A peaks provide the weighted mean $T(\theta)$ of the temperatures, from which we can deduce the parallel temperature. As

TABLE I: Experimental measurements of the parallel and perpendicular temperatures of the seeded gas. The fluorescence signal intensity gives a rough idea of the intensity of the lithium beam.

Source pressure (mbar)	$T_{\parallel 2}(K)$	$T_{\perp 2}(mK)$	Fluorescence signal(a.u.)
200	10.1	493	8.5
267	7.6	514	7.9
250	6.6	497	7.0
333	6.0	488	5.8
467	6.1	546	6.6
534	6.0	593	5.0
600	5.3	550	5.6

we think that our measurement may overestimate the perpendicular temperature, we have neglected the contribution of the perpendicular temperature when extracting the parallel temperature from $T(\theta)$, i.e. we have used:

$$T_{\parallel} = T(\theta)/\cos^2\theta \tag{49}$$

so that we get an upper limit of the parallel temperature $T_{\parallel}$. In table IV C, we have also given the fluorescence signal intensity in arbitrary units, as it gives an idea of the intensity of the lithium beam. The intensity decreases when the argon pressure increases. This behavior, which is not expected, may indicate some interaction of the beam with the residual gas, probably near the skimmer. The measured parallel temperature is plotted as a function of argon pressure in figure 4. We have also plotted the predicted theoretical dependence $T_{\parallel 2} = 0.31 \times T_{\parallel 1}$, where $T_{\parallel 1}$ is given by equations (29) and (30), using the semi-empirical coefficients of BV. The factor 0.31 which is the result of our theoretical calculation explains quite well our observations as long as the argon pressure is smaller than 400 millibar. For larger pressures, the parallel temperature remains constant while the theory predicts that it should still decrease. We tentatively assume that this discrepancy may be due to the interaction of the beam with the residual gas discussed above.

We will not recall here the data obtained by D. Pritchard and coworkers [23, 24] with a beam of sodium seeded in argon: this data, which has already been discussed in our previous paper [1], is also in agreement with our theoretical analysis.

V. CONCLUSION

In a previous letter [1], we have given a first evidence and a brief theoretical explanation of a new anomalous cooling effect, which appears in a supersonic expansion, when a light atom is seeded in an heavier carrier gas. The present paper has completed this letter by describing the details of our theoretical analysis and by presenting a larger set of experimental data.

We have first recalled and discussed the theoretical calculation of the parallel temperature in supersonic expansions of a pure monoatomic gas. In a second step, we have described in detail our extension of this theory to supersonic expansions of a mixture of two monoatomic gases, in the high dilution limit. In particular, we have explained the approximations we have made to get analytical equations for the parallel and perpendicular temperatures of

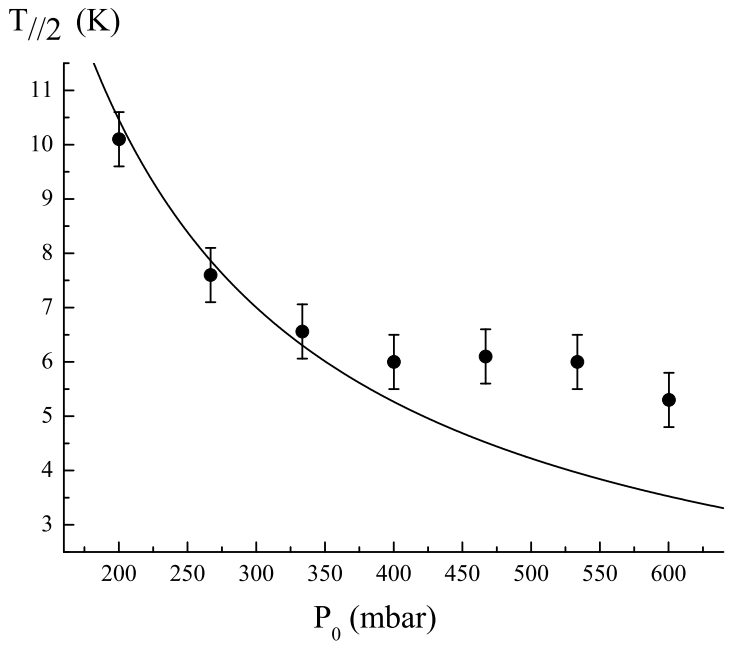

FIG. 4: The parallel temperature of lithium seeded in argon as a function of argon pressure in the source. The points represent our measurements while the full curve is the result of our theoretical calculation $T_{\|2} = 0.31 T_{\|1}$, where the argon parallel temperature is given by the semi-empirical law of Beijerinck and Verster. The agreement between theory and experiment is quite good when the argon pressure is below 400 millibar but, for larger source pressures, the lithium parallel temperature remains roughly constant, in disagreement with theory.

the seeded gas. We have integrated numerically the differential equations describing the parallel and perpendicular temperatures of the seeded gas and we have shown that these equations predict a large difference of terminal parallel temperatures for the carrier and seeded gases. The ratio of these two temperatures depends on several parameters, namely the ratio of the atomic masses of the two species and the ratio of their collision cross-sections at low temperature. We have deduced the lowest possible value of the temperature ratio $T_{\|2\infty}/T_{\|1\infty}$: this ratio may be quite small when a light species is seeded in a heavy species with $m_2 \ll m_1$.

In a last part, we have described a new set of measurements of the parallel velocity distribution of a supersonic beam of lithium seeded in argon, with a high dilution. The measured lithium parallel temperature is considerably lower than the calculated parallel temperature of the argon beam and the temperature ratio is in good agreement with our theoretical prediction, at least when the argon pressure is not too large. The deviation between theory and experiment, which appears at large argon pressures, is tentatively attributed to some interaction of the beam with the residual gas near the skimmer.

We think that the anomalous cooling effect described here is now well established. Several further studies would be very interesting. First of all, it should be easy to observe this effect in several simple experimental cases, a particularly striking one being molecular hydrogen seeded in argon. From the theoretical point of view, it should be possible to investigate this effect by other methods, including numerical simulation, and to estimate the effect of a

finite dilution.

As far as we know, this effect remained undetected up-to-now because it is rather unusual to seed a light atom in an heavier carrier gas. An other and very general interest of the present study is to emphasize that a supersonic expansion is not in thermal equilibrium and that some unexpected effects may result.

VI. ACKNOWLEDGEMENTS

We thank J.P. Toennies, H. C. W. Beijerinck, U. Buck and P. A. Skovorodko for helpful discussions. We also thank Ph. Dugourd and M. Broyer for advice concerning the design of the oven of our lithium supersonic beam, J. Schmiedmayer for advice concerning the use of LD688 dye as well as R. Delhuille, L. Jozefowski and C. Champenois for their important contributions to the development of this experiment. We thank Région Midi Pyrénées; IRSAMC and Université P. Sabatier for financial support.

VII. APPENDIX A: WEIGHTED CROSS-SECTIONS; THEIR DEFINITION AND CALCULATION OF THEIR TEMPERATURE DEPENDENCE

A. Definitions

We consider the collision between two atoms of species i and j with a relative velocity g and a reduced mass μ. The definitions and many results are taken from the book Molecular theory of gases and liquids, by Hirschfelder, Curtiss and Bird [25]. Starting from the differential cross-section $d\sigma_{i,j}(g)/d\Omega$, the angle-weighted cross-sections $Q^{(l)}_{i,j}(g)$ are defined by (equation 8.2-2 of [25]) :

$$Q^{(l)}_{i,j}(g) = \int \frac{d\sigma_{i,j}(g)}{d\Omega}(1-\cos^l\chi)d\Omega \tag{50}$$

where χ is the deflection angle. In classical mechanics, the deflection angle χ is a function of the impact parameter b and the relative velocity g. $Q^{(l)}_{i,j}(g)$ is then given by:

$$Q^{(l)}_{i,j}(g) = \int (1-\cos^l\chi)2\pi b db \tag{51}$$

The thermal averages $\Omega^{(l,s)}_{i,j}(T)$ are given by equation 8.2-3 of reference [25]:

$$\Omega^{(l,s)}_{i,j}(T) = \sqrt{k_B T/(2\pi\mu)}\int_0^\infty Q^{(l)}_{i,j}(g)\gamma^{2s+3}\exp(-\gamma^2)d\gamma \tag{52}$$

with $\gamma^2 = \mu g^2/(2k_BT)$.

The validity of classical mechanics to describe the collision at low energies may be questioned. Three circumstances contribute to make classical mechanics a good approximation in the experimental cases considered here:

- the quantum character of the interaction between two atoms is usually measured by the quantum parameter $\eta = \hbar^2/(m\sigma^2\epsilon)$ introduced by Stwalley and Nosanow [26] (see also De Boer and Lunbeck [27]) where ϵ is the potential well depth and σ the core

radius. A large value of η indicates a highly quantum behaviour while a small value corresponds to a quasi-classical behaviour. A highly quantum system is ^4He dimer with $\eta \approx 0.18$ [26]. As $\eta \approx 0.75 \times 10^{-3}$ for Ar dimer [30] and $\eta \approx 6.6 \times 10^{-3}$ for $^7Li - Ar$ interaction [29], these two systems have only a weak quantum character.

- the differential cross-section presents several types of quantum effects. These effects are largely reduced by the angle average following equation (50) and further reduced by the thermal average following equation (52).

- a quantum effect which survives these two averages is the behaviour of the cross-section at extremely low energy, in the quantum threshold regime. Following Julienne and Mies [28], this regime extends up to an energy of the order of $\hbar^3 \mu^{-3/2} C_6^{-1/2}$ for an potential with a C_6/r^6 long range. For instance, the quantum threshold effect explains the large increase of the helium-helium cross-section calculated by Toennies and Winkelmann. For argon-argon and lithium-argon collisions, using the C_6 of reference [32], we find that this regime could be observed for temperatures of the order of 10^{-2} and 2×10^{-2} Kelvin respectively, well below the lowest temperatures obtained in argon expansions, of the order of 1 Kelvin [5, 12].

B. Calculations with a Lennard-Jones $12-6$ potential

We consider an interaction potential of the $12-6$ Lennard-Jones type:

$$V(r) = \frac{C_{12}}{r^{12}} - \frac{C_6}{r^6} = 4\epsilon \left[\frac{\sigma^{12}}{r^{12}} - \frac{\sigma^6}{r^6} \right] \tag{53}$$

using the usual reduced quantities (see paragraph 8.2 of [25]). In a first step, we have calculated the deflection function $\chi(b)$ as a function of the reduced energy $E^* = \mu g^2/(2\epsilon)$, by numerical integration. Our calculation reproduces well the analytic deflection function of BV for $E^* \leq 0.1$ (see [5], appendix A), but the shape of this function varies with the energy and in particular, if $E^* > 0.8$, the orbiting singularity disappears.

We have then calculated the $Q^{(l)}(g)$ cross-sections with $l = 1$ and $l = 2$ as a function of E^*. In the low-energy range, $E^* \ll 1$, these two cross-sections are well approximated by an $(E^*)^{-1/3}$ behavior and, to make this behavior very clear, we have plotted in figure 5 the variation of $Q^{(l)}(g)E^{*1/3}$ as a function of E^*. At low energy, our calculation presents a small numerical noise associated to the orbiting singularity. We have not tried to reduce this noise by introducing some analytic approximations of the function $\chi(b)$ near this singularity.

When $E^* \longrightarrow 0$, we get:

$$Q^{(1)}(g) \approx (7.81 \pm 0.01)\sigma^2 E^{*-1/3} \tag{54}$$

and

$$Q^{(2)}(g) \approx (5.95 \pm 0.01)\sigma^2 E^{*-1/3} \tag{55}$$

Then, we have calculated numerically the $\Omega^{(l,s)}$ integrals as a function of the reduced temperature $T^* = k_B T/\epsilon$ and we have verified their low energy limits analytically (this is

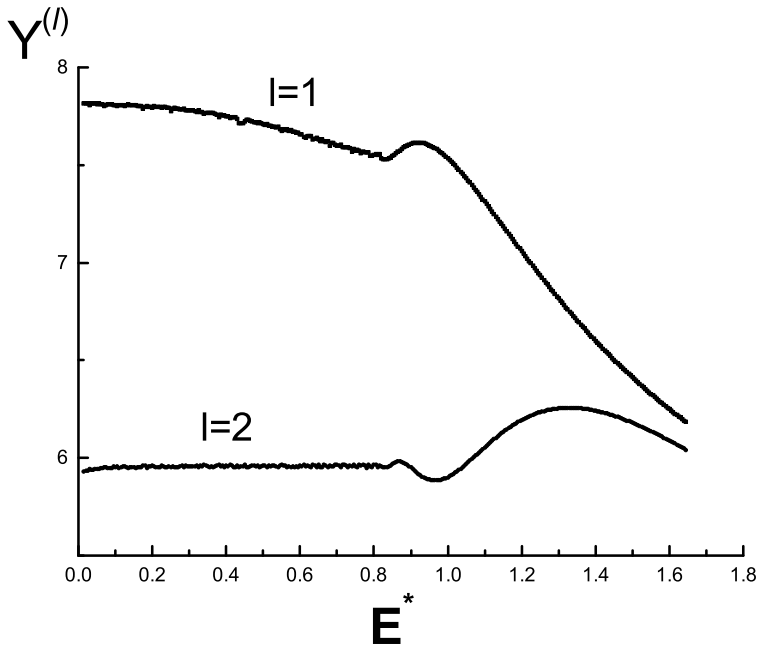

FIG. 5: Plot of the variations of $Y^{(l)} = Q^{(l)}(g)E^{*1/3}/\sigma^2$ as a function of E^* for $l = 1$ (upper curve) and $l = 2$ (lower curve). Both quantities approach their limit rapidly when $E^* < 0.5$.

easy as the integral in equation (52) can be expressed by a Gamma function). The various $\Omega^{(l,s)}(T)$ take a form analogous to equation (15):

$$\Omega^{(2,2)}(T) = C^{(l,s)}(T^*) \left(\frac{k_B T}{\mu}\right)^{1/2} \left(\frac{C_6}{k_B T}\right)^{1/3} \tag{56}$$

We have plotted in figure 6 the variations of three functions $C^{(l,s)}(T^*)$. We are mostly interested in their low-temperature limits, which are necessary for our calculations. We thus obtain $C^{(2,2)}(0) = 3.00$, in excellent agreement with BV result [5], $C^{(1,2)}(0) = 3.94$ and $C^{(1,1)}(0) = 1.48$. We have verified these results analytically (this is easy, using equations (54,55), the integral in equation (52) being expressed by a Gamma function). We also get the value of the ratio $\rho_o = C^{(1,2)}(0)/C^{(2,2)}(0) = 1.312 \pm 0.004$, also in very good agrement with the value $\rho_o = 1.32$ deduced from the analytic deflection function of BV [5].

VIII. APPENDIX B: CALCULATION OF $\mathbf{F}_{\parallel,2}$ AND $\mathbf{F}_{\perp,2}$

We want to calculate:

$$\mathcal{F}_{X,2} \approx \frac{n_1}{k_B u_\infty} \int \langle g \frac{d\sigma(g)}{d\Omega} \rangle d\Omega \int \Delta E_{X,2} f_1(\mathbf{v}_1) f_2(\mathbf{v}_2) d^3\mathbf{v}_1 d^3\mathbf{v}_2 d\Omega \tag{57}$$

with $X = \parallel$ and $\perp$. We introduce the center of mass velocity $\mathbf{v}_{cm}$

$$\mathbf{v}_{cm} = \alpha \mathbf{v}_1 + \beta \mathbf{v}_2 \tag{58}$$

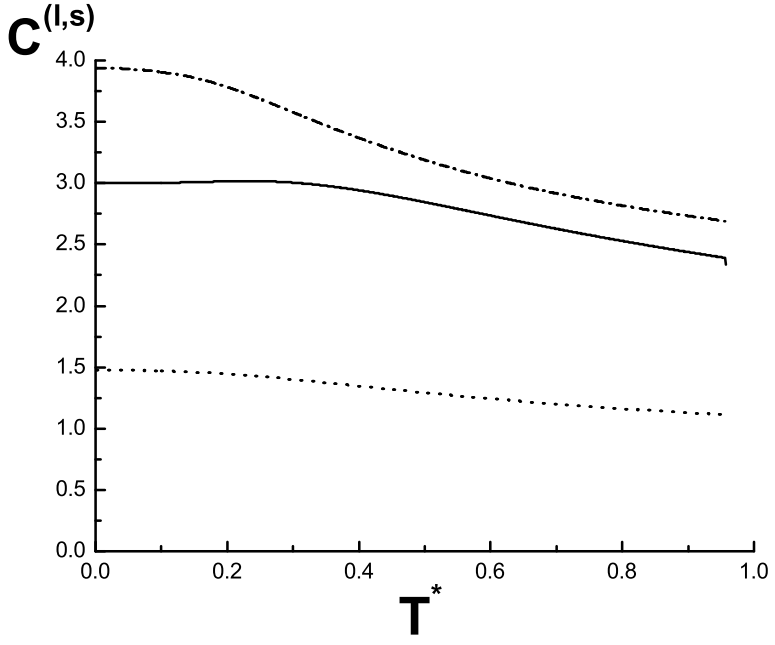

FIG. 6: Plot of the variations of the quantities $C^{(l,s)}(T^*)$ defined by equation (56) as a function of $T^* = k_B T/\epsilon$ for $(l,s) = (1,1)$ (dots); $(1,2)$ (dash-dotted curve) and $(2,2)$ (solid curve).

with $\alpha = m_1/M$, $\beta = m_2/M$ and $M = m_1 + m_2$. The relative velocity $\mathbf{g} = \mathbf{v}_1 - \mathbf{v}_2$ has already been introduced. The z axis is parallel to the hydrodynamic velocity and, to simplify the geometry, we may choose the x and y axis so that the initial relative velocity $\mathbf{g}$ lies in the yz plane, making an angle θ with the z axis. However, this choice complicates the following part of the calculation as it creates a correlation between the x-components of $\mathbf{v}_1$ and $\mathbf{v}_2$. We may eliminate this unphysical correlation by expressing the results as a function of the parallel and perpendicular components of the initial velocities, without any reference to their x,y components.

The relative velocity after the collision is noted $\mathbf{g}_f$. The deflection angle noted χ is the angle between $\mathbf{g}$ and $\mathbf{g}_f$. We must also introduce the azimuth φ measuring the orientation in space of the plane $\mathbf{g}$, $\mathbf{g}_f$. This azimuth φ is equally probable in the $0 \leq \varphi < 2\pi$ range. The final velocity of atom 2 is given by:

$$\mathbf{v}_{2f} = \alpha \mathbf{v}_1 + \beta \mathbf{v}_2 - \alpha \mathbf{g}_f \tag{59}$$

We express its parallel and perpendicular components as a function of the initial velocities, of the relative velocity and of the angles θ, φ and χ and we want to calculate:

$$\Delta E_{2X} = \frac{m_2}{2}\left(\mathbf{v}_{2fX}^2 - \mathbf{v}_{2X}^2\right) \tag{60}$$

We must then integrate these quantities over several variables:

- we first integrate over φ because this integration cancels several terms
- we then integrate over $\mathbf{v}_1$ and $\mathbf{v}_2$ with the normalized functions $f_1(\mathbf{v}_1) f_2(\mathbf{v}_2)$. All the terms involve double products of the type $v_{iX} v_{jY}$, where i, j stands for atom indices

$1, 2$ and X, Y for $\parallel$ or $\perp$. After integration, all these products vanish, excepted the ones with $i = j$ and $X = Y$ and their values are simply related to the temperature associated to this atom and this degree of freedom. We thus obtain:

$$\begin{aligned}\Delta E_{2\parallel} &= \frac{m_2}{2}\left[\frac{k_B T_{\parallel 1}}{m_1}\alpha^2\left(1-\cos\chi\right)^2 - \frac{k_B T_{\parallel 2}}{m_2}\left(\alpha^2\sin^2\chi + 2\alpha\beta\left(1-\cos\chi\right)\right)\right.\\ &+ \left.\left(\frac{k_B T_{\perp 1}}{m_1} + \frac{k_B T_{\perp 2}}{m_2}\right)\alpha^2\sin^2\chi\right] \qquad (61)\end{aligned}$$

$$\begin{aligned}\Delta E_{2\perp} &= \frac{m_2}{2}\left[\left(\frac{k_B T_{\parallel 1}}{m_1} + \frac{k_B T_{\parallel 2}}{m_2}\right)\alpha^2\sin^2\chi + \frac{k_B T_{\perp 1}}{m_2}\alpha^2\left(3+\cos^2\chi - 4\cos\chi\right)\right)\\ &- \left.\frac{k_B T_{\perp 2}}{m_2}\left(4\alpha\beta\left(1-\cos\chi\right) + \alpha^2\sin^2\chi\right)\right] \qquad (62)\end{aligned}$$

- we must finally integrate over the angle χ. The integrals involve the angular weights $(1-\cos^l\chi)$ with $l = 1$ and 2 only, i.e. they involve only $Q^{(1)}_{1,2}$ and $Q^{(2)}_{1,2}$ defined by equation (50). There was no terms involving $l = 1$ terms in the pure gas case. This new feature is due to the fact that the forward-backward symmetry existing in the pure gas case is now broken by the different masses of the two colliding atoms and by the fact that we calculate the energy transfer for atom 2 only.

- we have made an approximation by considering $gQ^{(l)}_{1,2}(g)$ as independent of g and we must fix its value. To be coherent with the pure gas case, we have made the same approximation in the pure gas case and we have identified the equations thus obtained with equations (14). We thus get:

$$\langle gQ^{(l)}_{1,2}(g)\rangle = \frac{32}{15}\Omega^{(l,2)}_{1,2}(T_m) \qquad (63)$$

  In our calculations, we have used $T_m = (T_{\parallel 1} + 2T_{\perp 1})/3$, which might not be the best choice. However, as $\Omega^{(l,2)}_{1,2}(T_m)$ varies very slowly, like $T_m^{1/6}$, we think that the exact choice for T_m has little influence on the result.

[1] A. Miffre, M. Jacquey, M. Büchner, G. Trénec and J. Vigué, accepted for publication in Phys. Rev. A, ArXiv.org/abs/physics/0401019
[2] J. B. Anderson and J. B. Fenn, Phys. Fluids **8**, 780 (1965)
[3] B. B. Hamel and D. R. Willis, Phys. Fluids, **9**, 8289 (1966)
[4] J. P. Toennies and K. Winkelmann, J. Chem. Phys. **66**, 3965 (1977)
[5] H. C. W. Beijerinck and N. F. Verster, Physica **111C**, 327 (1981)
[6] J. B. Anderson, Entropie **18**, 33 (1967)
[7] P. Raghuraman, P. Davidovits, and J. B. Anderson, Rarefied Gas Dynamics 10th Symposium, Aspen, 1976 (J. L. Potter editor, AIAA) Progress in Astronautics and Aeronautics, **51-1** 79 (1977)
[8] D. R. Miller, in Atomic and molecular beam methods, G. Scoles ed., p. 14-53 (Oxford University Press 1988)
[9] H. C. W. Beijerinck, P. Menger and N. F. Verster, Rarefied Gas Dynamics 11th symposium, R. Campargue ed. (CEA Paris) vol. 2, p 871 (1979)
[10] D. R. Miller and R. P. Andres, in Rarefied Gas Dynamics, L. Trilling and H. Y. Wachman eds. (Academic Press, New York) vol 2, p. 1385 (1969)
[11] U. Buck, H. Pauly, D. Pust and J. Schleusener, in Rarefied Gas Dynamics 9th symposium, M. Becker and M. Fiebig eds. (DFVLR-Press, Porz-Wahn) vol. 2, C.10 (1974)
[12] H. D. Meyer, MPI für Strömungforschung, Bericht 5 (Göttingen, 1978)
[13] H. L. Kramer and D. R. Herschbach, J. Chem. Phys. **53**, 2792 (1970)
[14] N. Takahashi and K. Teshima, in Rarefied Gas Dynamics 14th Symposium, H. Oguchi ed. (University of Tokyo Press) vol 2, p. 703 (1984)
[15] P. A. Skovorodko, private communication (January 2004)
[16] G. A. Bird, Molecular dynamics and the direct simulation of gas flows, Oxford University Press, Oxford (1994)
[17] P. A. Skovorodko, abstract submitted to Rarefied Gas Dynamics 24th Symposium (July 2004)
[18] R. Delhuille, C. Champenois, M. Büchner, L. Jozefowski, C. Rizzo, G. Trénec and J. Vigué, Appl. Phys. **B 74**, 489 (2002)
[19] J. Blanc et al., J. Chem. Phys. **96**, 1793 (1992)
[20] C. J. Sansonetti, B. Richou, R. Engleman Jr and L. J. Radziemski, Phys. Rev. A **52**, 2682 (1995)
[21] W. I. McAlexander, E. R. I. Abraham and R. G. Hulet, Phys. Rev. A **54**, R5 (1996)
[22] T. W. Hänsch and B. Couillaud, Opt. Comm. **35**, 441 (1980)
[23] J. Schmiedmayer, M. S. Chapman, C. R. Ekstrom, T. D. Hammond, D. A. Kokorowski, A. Lenef, R.A. Rubinstein, E. T. Smith and D. E. Pritchard, in Atom interferometry edited by P. R. Berman (Academic Press 1997), p 1
[24] C. R. Ekstrom, J. Schmiedmayer, M. S. Chapman, T. D. Hammond and D. E. Pritchard, Phys. Rev. A **51**, 3883 (1995)
[25] J. O. Hirschfelder, C. F. Curtiss and R. B. Bird, Molecular theory of liquids, (Wiley, New York, 1954)
[26] W.C. Stwalley and L. H. Nosanow, Phys. Rev. Lett. **36**, 910 (1976)
[27] J. De Boer and R.J. Lunbeck, Physica **XIV**, 520 (1948)
[28] P. S. Julienne and F. H. Mies, J. Opt. Soc. Am. **B 6**, 2257 (1989)

[29] R. Brühl and D. Zimmermann, Chem. Phys. Lett. **233**, 455 (1995)
[30] R. A. Aziz, J. Chem. Phys. **99**, 4518 (1993)
[31] K. T. Tang and J. P. Toennies, J. Chem. Phys. **118**, 4976 (2003)
[32] K. T. Tang, J. M. Norbeck and P. R. Certain, J. Chem. Phys. **64**, 3063 (1976)